Impedance Spectroscopy and Phase Structure of Polyether−Poly(methyl methacrylate)−$LiCF_3SO_3$ Blend-Based Electrolytes

W. Wieczorek and J. R. Stevens*

Department of Physics University of Guelph, Guelph, Ontario, Canada N1G 2W1

Received: August 14, 1996; In Final Form: November 15, 1996[⊗]

Polymeric electrolytes obtained by the free radical polymerization of methyl methacrylate in a solution of $LiCF_3SO_3$ in an ethylene oxide−propylene oxide copolymer are studied. These electrolytes exhibit ambient temperature conductivities up to 3×10^{-5} S/cm. Impedance spectroscopy experiments performed in a symmetrical cell with two lithium electrodes show that the properties of lithium electrode−polymer electrolyte interface are improved after the *in situ* polymerization of methyl methacrylate in the electrolyte. The growth of the resistance of the passive layer formed on the electrode−electrolyte interface is suppressed. The impedance studies are coupled with FT-IR measurements which show that the fraction of contact-ion pairs is reduced in electrolytes for which limited growth of the resistance of the passive layers is observed.

Introduction

A driving force in the investigation and development of new polymeric electrolytes is the possibility of their application in various electrochemical devices.[1−5] Much effort has gone into the enhancement of the ionic conductivity at ambient and subambient temperatures for polyether-based electrolytes—the most intensively studied systems.[1−5] Novel polymeric ionic conductors such as composites,[3−6] networks,[7] and gels[8] have been synthesized and their structure−conductivity characteristics have been discussed. The electrochemical stability of polymeric electrolytes in contact with alkali metal electrodes, primarily lithium, and the compatibility of these electrolytes with electrode materials is also very important in electrochemical devices.[9−15] It was recognized[9−11] that a passive layer whose resistance increases with time is formed between a lithium electrode and a polymeric electrolyte. The structure of this layer is not understood, but it is known that uncontrolled passivation phenomena affect the cyclability of lithium electrodes and therefore the entire lithium battery.[13−16] It is suspected that the nature of this layer depends largely on the composition and purity of the electrolyte. The layer, having properties of a solid lithium ionic conductor with a high electrical resistance, acts as a solid phase between the lithium and the electrolyte. It has been demonstrated by Scrosati and co-workers[14−16] that the addition of inorganic fillers, such as $LiAlO_2$ or zeolites, improves electrode−electrolyte compatibility and reduces the passivation phenomena. This has been attributed to the effect of such fillers on polymer matrix impurities (*e.g.,* moisture or low molecular weight volatile solvents), which are suspected to react with lithium leading to the formation and growth of these passive layers. Recently it has been reported by Borkowska *et al.*[12] that the growth of the resistance of passive layers is limited for blend-based poly(ethylene oxide) (PEO)−$LiClO_4$ electrolytes with various methacrylic and acrylic polymers used as additives. Even stronger effects of poly(methyl methacrylate) (PMMA) on the stabilization of electrode−electrolyte interface have been reported by Scrosati *et al.*[13] for a variety of PMMA-based gel electrolytes. The latter systems were based on solutions of lithium salts in a propylene carbonate −ethylene carbonate mixture. It was shown that the growth of the resistance of passive layers is almost suppressed in these systems.

In the present paper the effect of *in situ* polymerized MMA on the characteristic of lithium−polymer electrolyte interface is studied for blend-based electrolytes obtained by the polymerization of methyl methacrylate (MMA) in a polyglycol−$LiCF_3SO_3$ matrix. We decided to use a medium molecular weight ($M_w = 2600$) ethylene oxide (EO)−propylene oxide (PO) copolymer (which is in the form of a viscous liquid) due to the ease of purification. The effect of the PMMA concentration on the conductivity and electrode−electrolyte resistance is discussed on the basis of impedance spectroscopy data obtained in a symmetrical cell with two lithium electrodes. Structural characteristics of these electrolytes have been studied by FT-IR and thermal characteristics by differential scanning calorimetry (DSC). Li^+ transport numbers have been evaluated at 80 °C on the basis of an impedance method developed by Sorensen and Jacobssen.[17]

Experimental Section

Sample Preparation. EO−PO copolymer ($M_w = 2600$, 50% of EO monomeric units, and OH capped) was stringently freeze dried using freeze−pump−thaw cycles under reduced pressure (10^{-3} Torr). This was followed by drying the copolymer over molecular sieves type 4 Å under reduced pressure at 70 °C for about 72 h. Lithium triflate ($LiCF_3SO_3$) (97% Aldrich) was dried under vacuum for 48 h at 120 °C prior to use. MMA was dried and distilled over calcium hydride under reduced pressure. AIBN was recrystallized from methanol.

Polymer electrolytes were obtained by the following procedure.[18] While still under vacuum, the polyether was transferred to a glovebox maintained under an argon atmosphere (moisture content lower than 20 ppm) where $LiCF_3SO_3$ was directly dissolved under stirring at ∼40−50 °C. The polyether−$LiCF_3SO_3$ solution was then transferred to a polymerization vessel provided with a mechanical stirrer. The required amount of MMA with AIBN (1 mass %) was injected into the polymerization vessel and mixed thoroughly with the polyether and maintained at 60 °C for about 24 h. The polymerization reaction was carried out under an argon atmosphere. After the completion of the polymerization, these blend samples were pumped on (∼10^{-3} Torr) at 60 °C for about 72 h. This procedure was used to remove traces of unreacted monomer from the blend. The final composition of these blends was established on the basis of ^{1}H NMR measurements as described elsewhere.[18]

[⊗] Abstract published in *Advance ACS Abstracts,* February 1, 1997.

S1089-5647(96)02517-5 CCC: $14.00

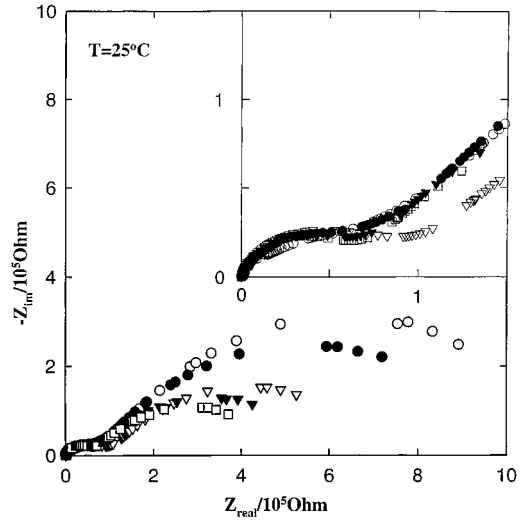

Figure 1. Impedance spectra registered for PEO−PPO−$LiCF_3SO_3$−PMMA (15 mass %) electrolyte in a symmetrical cell with metallic lithium electrodes. Spectra registered for different times of storage: [○] 1 day, [●] 3 days, [▽] 4 days, [▼] 8 days, [□] 10 days. The inset in the upper right shows an amplification of the high-frequency semicircles.

Samples containing up to 5 mass % of PMMA were in the form of viscous liquids, whereas those with higher PMMA content were viscoelastic solids.

DSC Studies. DSC data were obtained between −110 and 100 °C using a DuPont TA 2910 scanning calorimeter with a low-temperature measuring head and liquid-nitrogen-cooled heating element. Approximately 10−20 mg samples in aluminum pans were cooled to −110 °C and then heated at 10 °C min^{-1} to a final temperature of 100 °C.

FT-IR Spectroscopy. Infrared spectra were recorded on a computer-interfaced Nicolet FT-IR System 4.4 instrument in the frequency range 4000−400 cm^{-1} with a wavenumber resolution of 2 cm^{-1}. All FT-IR experiments were performed at 25 ± 1 °C. Thin film electrolyte foils were sandwiched between two NaCl plates.

Impedance Spectroscopy Measurements. Impedance spectroscopy experiments were performed in the temperature range from 25 to 100 °C. Each electrolyte sample was sandwiched between two lithium electrodes. The lithium electrodes were made by cold-pressing lithium foil onto stainless steel disks just before cell assembly. All of the experiments with lithium were done in a dry atmosphere glovebox. The impedance cell was evacuated ($<10^{-4}$ Torr) before measurements were initiated. Impedance experiments were repeated several times for a period of 2 weeks. The impedance cell was stored under a static vacuum maintained throughout the experimental time period. Impedance experiments were carried out on a computer interfaced HP 4192 A impedance analyzer over the frequency range 5−13 MHz. The impedance cell was placed in a temperature-controlled furnace (temperature accuracy: ±1 °C). Impedance data were analyzed using a nonlinear least-squares fitting procedure developed by Boukamp.[19]

Results

Impedance Spectroscopy. Figure 1 is an example of impedance spectra obtained for the PEO−PPO−$LiCF_3SO_3$−PMMA (15 mass %) electrolyte at 25 °C during the storage of this electrolyte between two lithium electrodes under static vacuum over periods up to 10 days. Each spectrum consists of two distorted semicircles. The high-frequency semicircles registered for different times of storage approximately overlap

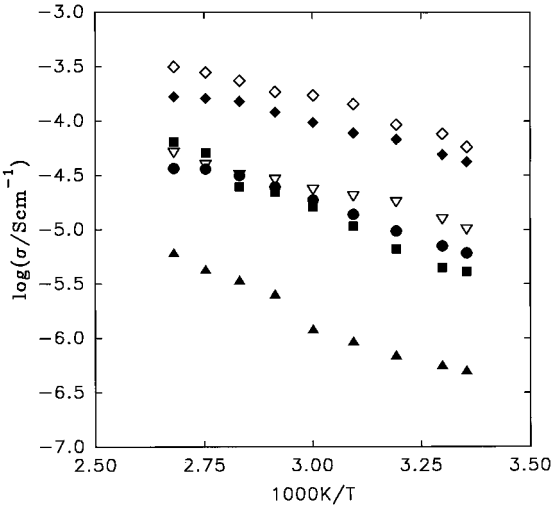

Figure 2. Ionic conductivity as a function of reciprocal temperature for PEO−PPO−$LiCF_3SO_3$−PMMA electrolytes after 1 day. Samples of various PMMA concentrations: [◇] 0 mass % PMMA, [◆] 5 mass % PMMA, [▽] 10 mass % PMMA, [●] 15 mass % PMMA, [■] 20 mass % PMMA, [▲] 30 mass % PMMA.

with each other. The values of capacitance calculated for the high-frequency semicircle varied between 10^{-11} and 10^{-12} F/cm^2 depending on temperature and sample composition. These values of capacitances are typical for bulk relaxation phenomena, and therefore, the high-frequency semicircle represents the bulk electrolyte response characteristic.[20] The electrolyte resistance (R_b) calculated from the span of the high-frequency semicircle is almost time independent for a particular sample composition at constant temperature.

Figure 2 shows changes of the logarithm of ionic conductivity (σ) as a function of inverse temperature where

$$\sigma = \frac{4a}{\pi d^2 R_b} \tag{1}$$

Here, a is the electrolyte thickness and d is the electrode diameter. The ambient temperature ionic conductivity decreases as the concentration of PMMA increases. Ambient temperature conductivities measured for samples containing up to 20 mass % of PMMA are all above 5×10^{-6} S/cm with the highest values approaching 3×10^{-5} S/cm for electrolytes with 0 and 5 mass % of PMMA. Conductivities measured for the electrolyte with 30 mass % of PMMA are about 1 order of magnitude lower than conductivities measured for the other solid electrolytes over the entire temperature range used. It can also be noticed that conductivities measured for liquid electrolytes (samples with 0 and 5 mass % of PMMA) are about 3−10 times higher than for electrolytes containing 10−20 mass % of PMMA.

As can be seen from Figure 1, the span of a second (low-frequency) semicircle varies with time. Over 10 days of sample storage the span decreases, and after two weeks of storage a small increase in the span of this semicircle is noticed. The capacitances calculated for this semicircle are almost time invariant, but an increase in capacitance is noticed with an increase in temperature for each composition of the electrolyte. These capacitances are typical of interfacial electrode−electrolyte phenomena[20] and can be associated with the formation of passive layers. Typical interfacial capacitances obtained at 25 and 100 °C are summarized in Table 1. They are all in the range 10^{-8}−10^{-7} F/cm^2, except for the samples with 10 mass % of PMMA for which ambient temperature capacitances are within the 10^{-9}−10^{-8} F/cm^2 range. The electrode−

TABLE 1: Interfacial Capacitancies (C_i) and E_a[a] Values for PEO−PPO−PMMA−$LiCF_3SO_3$ Blend-Based Electrolytes

sample compn	C_i (fcm^2) (25 °C)	C_i (fcm^2) (100 °C)	E_a (eV) (72 h)	E_a (eV) (240 h)
PEO−PPO−$LiCF_3SO_3$: 10 mass % PMMA	1.5×10^{-9}	1×10^{-8}	0.58	0.37
PEO−PPO−$LiCF_3SO_3$: 15 mass % PMMA	1.5×10^{-8}	4×10^{-8}	0.43	0.45
PEO−PPO−$LiCF_3SO_3$: 20 mass % PMMA	2×10^{-8}	1×10^{-7}	0.42	0.43
PEO−PPO−$LiCF_3SO_3$: 30 mass % PMMA	1×10^{-8}	4×10^{-8}	0.50	0.52

[a] E_a values calculated on the basis of eq 2. Symbols have the same meaning as in the text.

TABLE 2: Glass Transition Temperatures and Fraction of "Free" Anions for PEO−PPO−PMMA−$LiCF_3SO_3$ Blend-Based Electrolytes

sample compn	T_g (°C)	fraction of "free" anions (%)
PEO−PPO	−67	
PEO−PPO−$LiCF_3SO_3$	−56	60
PEO−PPO−$LiCF_3SO_3$: 5 mass % PMMA	−55	68
PEO−PPO−$LiCF_3SO_3$: 10 mass % PMMA	−54	68
PEO−PPO−$LiCF_3SO_3$: 15 mass % PMMA	−52	87
PEO−PPO−$LiCF_3SO_3$: 20 mass % PMMA	−52	92
PEO−PPO−$LiCF_3SO_3$: 30 mass % PMMA	−44	88

electrolyte interfacial resistances (R_i) can be calculated from the span of the low-frequency semicircles.

Figure 3 presents changes in the R_i as a function of time for viscoelastic electrolytes (samples with at least 10 mass % of PMMA) measured at 30 °C (Figure 3a), 70 °C (Figure 3b), and 100 °C (Figure 3c). As can be seen from these figures, similar trends were observed. R_i measured for the sample with 10 mass % of PMMA increases with time, whereas resistances measured for the other samples vary randomly but generally do not change by more than a factor of 2 over the entire time period. At 100 °C, R_i measured for samples containing more than 10 mass % of PMMA remains almost unchanged over the 14 days of study.

Figure 4 presents the temperature dependence of the reciprocal of the R_i as a function of inverse temperature measured after 72 h (Figure 4a) and after 240 h (Figure 4b). The inverse of R_i represents the change in the rate of the charge transfer reaction at the interface. After 72 h, R_i^{-1} measured for the sample with 20 mass % of PMMA was the highest, whereas after 240 h R_i^{-1} increased monotonically with an increase in the PMMA concentration. The temperature dependence of R_i^{-1} can be described by an Arrhenius-type dependence (eq 2) for each electrolyte composition.

$$R_i^{-1} = A \exp\left(\frac{-E_a}{k_B T}\right) \qquad (2)$$

Here A is a preexponential factor, E_a is an activation energy, and k_B is the Boltzmann constant. Values of activation energy calculated on the basis of eq 2 are summarized in Table 1. All E_a values are within the 0.3−0.6 eV range. For samples with more than 10 mass % of PMMA, E_a remains almost constant in time, whereas for the sample with 10 mass % of PMMA, E_a decreases with time.

DSC Studies. DSC curves registered for all of the samples studied did not display any first-order transitions over the entire temperature range. Therefore, it can be concluded that these samples are amorphous. The only transition observed was the glass transition of the polyether phase. The glass transition temperature (T_g) values are summarized in Table 2. T_g measured for the undoped EO−PO copolymer is equal to −67 °C and increases up to −56 °C after the addition of $LiCF_3SO_3$. This results from the formation of transient cross-links involving lithium cations and the polyether matrix. Further slight increases in T_g were noticed for the samples containing from 5 to 20 mass % of PMMA. A more pronounced increase in T_g (to −44 °C) was observed for the sample containing 30 mass % of PMMA.

FT-IR Studies. Figure 5 shows FT-IR spectra recorded between 1600 and 800 cm^{-1} for the EO−PO copolymer (Figure 5a), the EO−PO copolymer with 4 mol% of $LiCF_3SO_3$ (Figure 5b), and the blend-based electrolyte with 30 mass % of PMMA (Figure 5c). The C═O symmetric stretch region (∼1730 cm^{-1}), the C−O−C symmetric and antisymmetric stretch region (∼1100cm^{-1}), as well as vibrations of the $CF_3SO_3^-$ anions (∼1300−1200cm^{-1}) and (∼1030 cm^{-1}), were analyzed. The addition of $LiCF_3SO_3$ causes a small decrease (5−7 cm^{-1}) of the C−O−C stretch down to lower wavenumbers due to the coordination of the ether oxygen with the lithium cation. For samples containing PMMA, the position of C−O−C (polyether) and C═O modes varied randomly over a narrow range of 1106−1109 and 1730−1735 cm^{-1}, respectively. In the 1300−1200 cm^{-1} region, peaks around 1290 and 1250 cm^{-1} were observed for the EO−PO copolymer and a peak at 1225 cm^{-1} was observed upon the addition of the salt. The ∼1290 and ∼1250 cm^{-1} peaks are observed for undoped EO−PO copolymer and, according to literature, are assigned to CH_2 twisting vibrations.[21] The intensity of these peaks increases after the addition of $LiCF_3SO_3$, but their positions are relatively unchanged. The positions of these peaks overlap with the positions of the $\upsilon(SO_3)_a$ bands from coordinated triflate ions as quoted by previous studies.[22−24] The 1225 cm^{-1} band has been assigned previously to the $\upsilon(CF_3)_s$ vibrations of "free" triflate anions.[22−24] Also, the peak at 1272 cm^{-1} (indicative of free triflate ions) has not been resolved. It can be concluded that IR bands characteristic of triflate ion vibrations appearing between 1250 and 1300cm^{-1} are masked by more intensive polyether vibrations and that no quantitative information can be obtained from this region.[24]

In the symmetric SO_3 stretch region (∼1030−1040 cm^{-1}), the contributions from "free anions" (∼1032 cm^{-1}) and contact-ion pairs (∼1042 cm^{-1}) can be seen in Figures 5b,c. A Gaussian−Lorentzian function has been used to fit this region of the IR spectra.[25] (A polynomial function was used to fit the base line.) Examples of fits are presented in Figure 6 for the EO−PO−$LiCF_3SO_3$ electrolyte (Figure 6a) and for the blend-based electrolyte with 30 mass % of PMMA (Figure 6b). The fraction of free anions has been calculated as the ratio of the area under the peak with maximum at ∼1032 cm^{-1} to the total area of the $\upsilon(SO_3)_s$ envelope. The results are summarized in Table 2. The fraction of free anions increases from 60% for the EO−PO−$LiCF_3SO_3$ electrolyte to a range of 87−92% for samples containing more than 10 mass % of PMMA. This effect is similar to the effect of the addition of cryptand (in which the crown ether traps and isolates the Li^+) observed for poly(propylene glycol) (PPG)−$LiCF_3SO_3$ electrolytes.[22] The fraction of free anions calculated for the EO−PO−$LiCF_3SO_3$ electrolyte is slightly lower than the value 0.75 calculated by Torell and co-workers for poly(ethylene glycol) (PEG) (M_w=400 and OH capped)−$LiCF_3SO_3$ electrolytes.[23] This results from the lower concentration of OH groups in our electrolytes; not all of the $CF_3SO_3^-$ anions can be bonded to the end OH groups as was the case for Torell's system.[23] However, the fraction of free anions is still much larger than that reported by Torell *et al.*[23] for the PEG (OCH_3 capped)−$LiCF_3SO_3$ electrolyte.

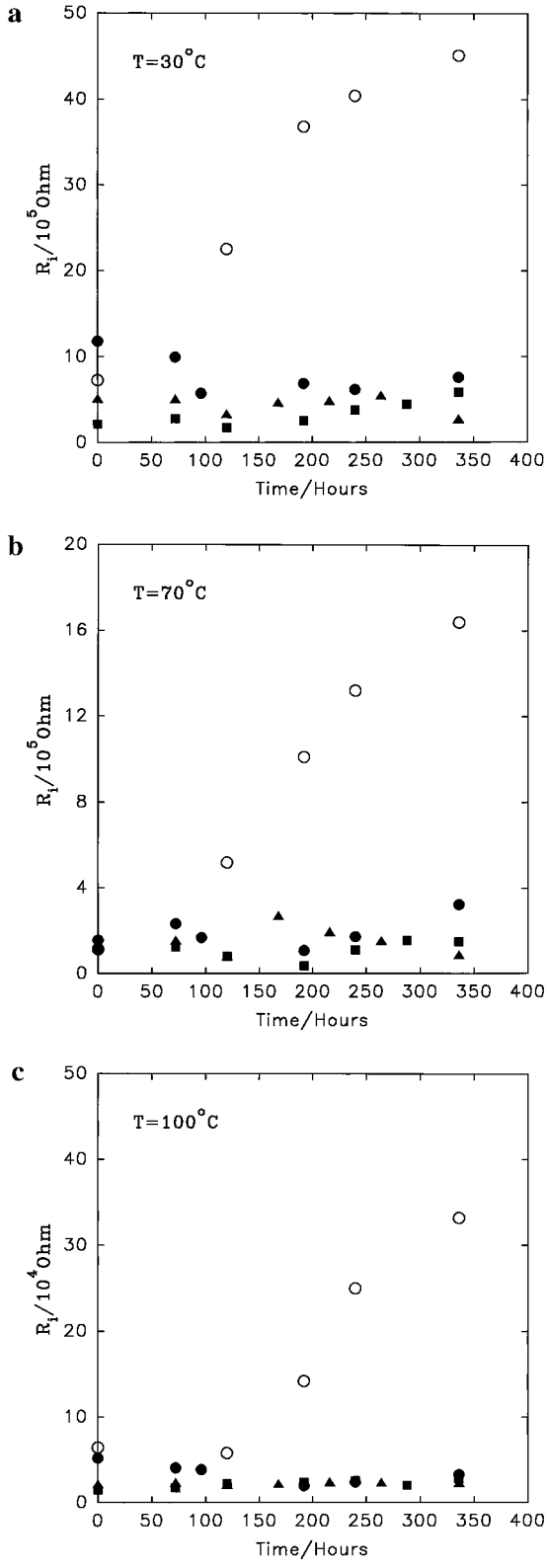

Figure 3. R_i as a function of time for PEO−PPO−$LiCF_3SO_3$−PMMA electrolytes. Data obtained at (a) 30 °C, (b), 70 °C, and (c) 100 °C. Samples of various PMMA concentrations: [○] 10 mass % PMMA, [●] 15 mass % PMMA, [■] 20 mass % PMMA, [▲] 30 mass % PMMA.

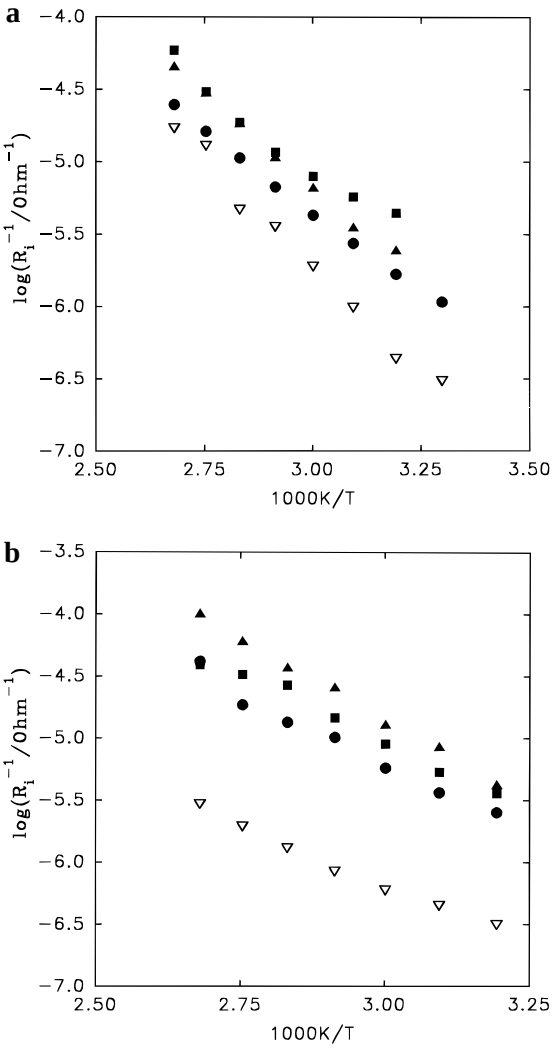

Figure 4. R_i as a function of inverse temperature for PEO−PPO−$LiCF_3SO_3$−PMMA electrolytes. Samples of various PMMA concentrations: (a) 3rd day of experiments, (b) 10th day of experiments; [▽] 10 mass % PMMA, [●] 15 mass % PMMA, [■] 20 mass % PMMA, [▲] 30 mass % PMMA.

Discussion

Blend-based EO−PO−PMMA−$LiCF_3SO_3$ electrolytes are either viscous liquids (samples with up to 5 mass % of PMMA) or viscoelastic solids in which liquid polyether is trapped in the PMMA matrix. On the basis of the T_g data presented in Table 2, it is suggested that the PMMA has little influence on T_g and, therefore, that the PMMA and polyether phases are microphase separated in spite of the visible homogeneity of these systems. The T_g values are almost constant for samples of various PMMA concentrations except for the electrolyte with 30 mass % of PMMA. These observations are in agreement with previous work on similar systems.[26,27] Ionic conductivity in these blend-based electrolytes decreases with an increase in the PMMA concentration as well as with an increase in T_g. This is consistent with previous results on a PPG (2000)−PMMA system where the ambient temperature conductivity decreased from 6.4×10^{-6} to 4.9×10^{-6} S/cm with an increase in PMMA concentrations from 4 to 8 mass %. The conductivities in the present study are higher than those in the PPG (2000)−PMMA system because of the presence of EO segments. Conductivities measured for liquid electrolytes (samples with 0 and 5 mass % of PMMA, see Figure 2) are about 3−10 times higher than those for solid electrolytes containing up to 20 mass % of PMMA and about 2 orders of magnitude higher than conductivities of the sample with 30 mass % of PMMA.

FT-IR studies indicate that the addition of PMMA results in an increase in the fraction of free anions which approaches 90% for electrolytes with more than 10 mass % of PMMA. One possibility for the increase in the fraction of free anions is the complexation of Li^+ cations by the ester group of PMMA which

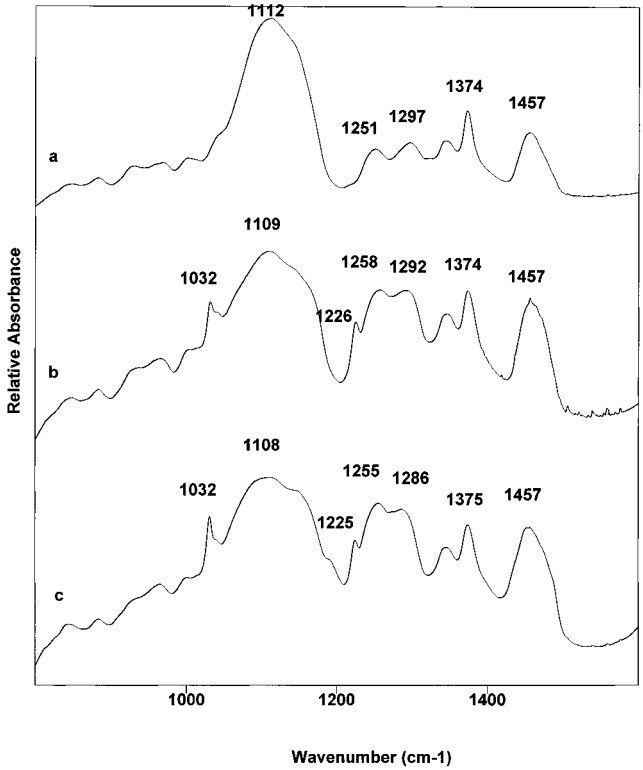

Figure 5. Exemplary FT-IR spectra registered at 25 °C in the wavenumber range 1600−800 cm^{-1} for (a) PEO−PPO copolymer, (b) PEO−PPO−$LiCF_3SO_3$ electrolyte, (c) PEO−PPO−$LiCF_3SO_3$−PMMA electrolyte (30 mass % PMMA).

facilitates the visual homogeneity through transient cross-linking of the ester groups and the ether oxygen of the EO−PO copolymer.

The most important finding arising from these studies is the effect of PMMA on the interfacial resistance (R_i) between the lithium electrodes and the EO−PO−PMMA−$LiCF_3SO_3$ electrolyte. For liquid electrolytes (<10 mass % of PMMA), R_i increases with time and results obtained for these systems are not discussed further since similar trends to those reported previously for other polymeric electrolytes[9−11] have been observed. However, it has been shown that the addition of at least 15 mass % of PMMA stabilizes the magnitude of R_i. As has been discussed before,[10,11] the formation of passive layers is most probably a two-step process. The first step in our system is the formation of the "primary" film with initial resistance R_i and is most probably due to a chemical reaction between the OH polymer end groups and metallic lithium. For other systems, the initial resistive properties of the primary film could be due to the reaction of the lithium electrode with electrolyte impurities.[11] We have intentionally used hydroxyl-terminated polyether chains to help us with the monitoring of the behavior of the electrode−electrolyte interface. After the completion of the formation of the primary film, the second step involves the formation of a "secondary" film which develops over time. As has been pointed out in previous studies, the chemical properties of the secondary film reflect the chemical properties of the electrolyte and therefore this secondary film is often referred to as a solid electrolyte interface (SEI).[10,28] As has been demonstrated by Fauteaux,[10] the properties of this film depend on electrolyte composition, salt concentration, and the transference numbers of the ions.

In EO−PO−$LiCF_3SO_3$−PMMA systems (samples with more than 10 mass % of PMMA), the formation of a secondary film is either not observed or is limited. Thus, the effect of the addition of PMMA is similar to that observed by Borkowska *et al.*[12] for polyether−polyacrylate blends and by Scrosati and coworkers for composite electrolytes containing zeolites or $LiAlO_2$[14−15] or in PMMA-based gels.[13] However, in none of the previous studies in which authors have observed the effect of PMMA on the behavior of the Li−polymer electrolyte interface was any explanation of the phenomena proposed. We would like to emphasize that the stabilization of R_i occurs for electrolytes for which an increase in the fraction of free anions

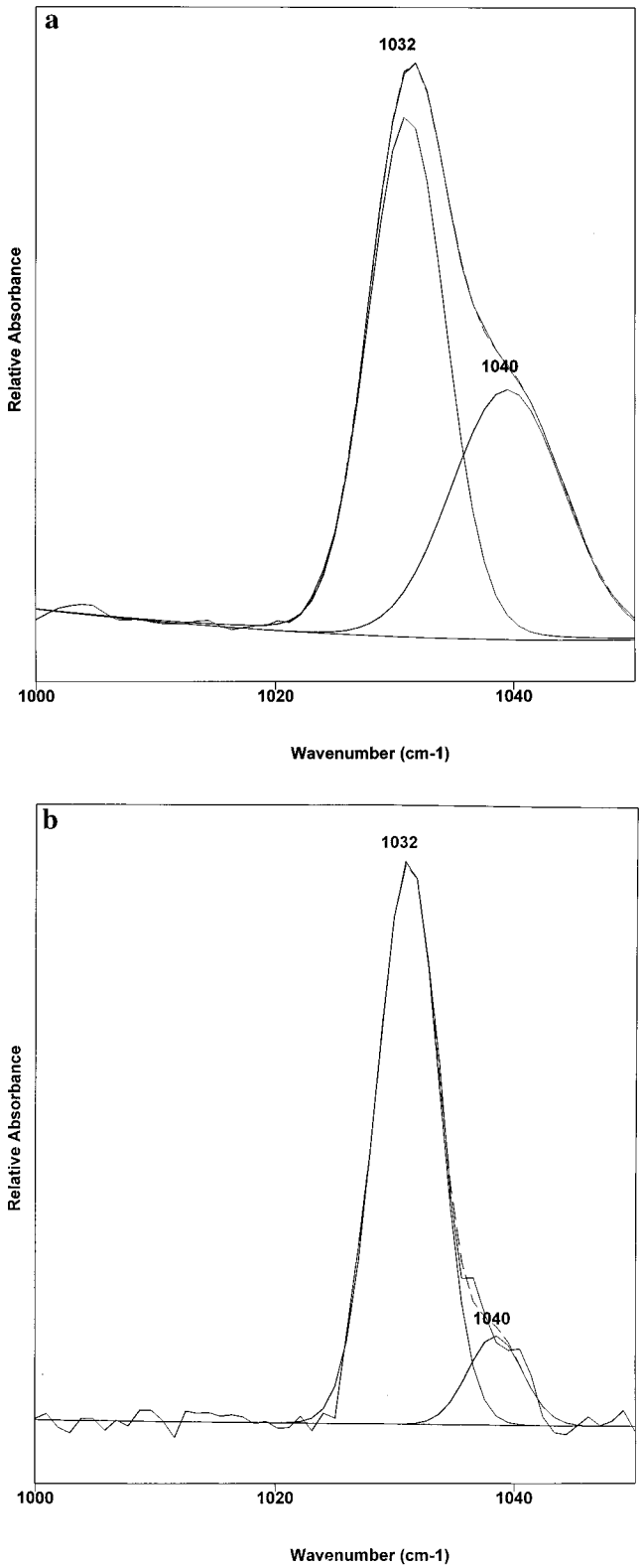

Figure 6. Peak fitting for the $\upsilon(SO_3)_s$ FT-IR region for the (a) PEO−PPO−$LiCF_3SO_3$ electrolyte, (b) PEO−PPO−$LiCF_3SO_3$−PMMA (30 mass %) electrolyte at 25 °C.

has been observed. It can result in a reduction of any "anionic cloud" formed close to an electrode−electrolyte interface which blocks the diffusion of Li^+ cations to and from the electrode. The mobility of free anions is higher than that of contact-ion pairs or negatively charged higher aggregates, and therefore, the possibility of the formation and buildup of clusters of negatively charged species as an anionic cloud close to the lithium electrode should be lower. The importance of the formation of contact-ion pairs on the electrode−electrolyte characteristics has been recently emphasized by Calhoun and Voth.[29] These authors demonstrated using molecular dynamics simulations that the free energy barrier for interfacial (aqueous electrolyte−electrode) electron transfer increases with a decrease in the cation−anion separation. It has also been shown[29] that the solvent reorganization energy is significantly increased for systems with contact-ion pairs. Similar effects involving an increase in the fraction of free anions have been previously observed for a variety of composite electrolytes,[6,30] and we suspect it should also occur for the composite systems studied by Scrosati *et al.*[14,15] It can be concluded from the values of C_i (Table 1) that the thickness of the interface layer decreases for samples with more than 10 mass % of PMMA; C_i decreases with an increase in PMMA content assuming the same electrode active area.

In lithium batteries there are three stages during the discharge of a lithium electrode covered by a SEI film:[31] (1) oxidation of lithium at the phase boundary lithium−SEI, (2) migration of Li^+ through the SEI film, (3) Li^+ transfer into the polymer electrolyte phase at the SEI−electrolyte interface. One of these stages limits the rate of the charge transfer reaction. On the basis of the E_a values (see Table 1), it is suggested that step 2 is the limiting stage for charge transfer across the electrode−electrolyte interface in this study.

The other possibility which can explain the stabilization effect of the addition of PMMA is the reaction of lithium cations with the ester groups of PMMA and the formation of a protective layer close to the electrode−electrolyte interface. The effect of this layer would be to protect Li from the impurities (including moisture) present in the electrolyte, and therefore, it would be similar to the role attributed by Scrosati[14,15] to zeolites or $LiAlO_2$ in his composite electrolytes or to the dramatic improvement in the stability of polyether−PMMA−$LiCF_3SO_3$ electrolytes toward atmospheric moisture.[18,26,27,32] As has been found from the transport number investigation using the Sorensen and Jacobsen impedance method,[17] the presence of PMMA does not change cation transport numbers, which for all of the electrolytes studied have been in the range of 0.3 ± 0.05; the values were measured at 80 °C.

Conclusions

Blend-based polymer electrolytes obtained by the *in situ* polymerization of MMA in a solution of $LiCF_3SO_3$ in EO−PO copolymer have been studied. The conductivity of these electrolytes decreases with an increase in PMMA concentration with the highest values approaching 10^{-5} S/cm at ambient temperatures. The addition of PMMA lowers the concentration of contact-ion pairs as compared to the pure EO−PO−$LiCF_3SO_3$ electrolyte and limits the effects of impurities such as moisture on the polymer electrolyte−lithium electrode interface. A significantly reduced rate of growth of R_i is observed in the presence of PMMA incorporated by the *in situ* polymerization of MMA.

Acknowledgment. We gratefully acknowledge financial support from an Industry Oriented Research Grant from the Natural Sciences and Engineering Council of Canada.

References and Notes

(1) Vincent, C. A. *Prog. Solid State Chem.* **1987**, *17*, 145.
(2) For instance, see: *Polymer Electrolyte Reviews*; MacCallum, J. R., Vincent, C. A., Eds.; Elsevier: London, 1987, Vol. 1; 1989, Vol. 1.
(3) Gray, F. M. *Solid Polymer Electrolytes-Fundamentals and Technological Applications*; VCH: Weinhem, Germany, 1991.
(4) *Applications of Electroactive Polymers*; Scrosati, B., Ed.; Chapman and Hall: London, 1993.
(5) Bruce, P. *Solid State Electrochemistry*; Cambridge University Press: Cambridge, 1995.
(6) Wieczorek, W.; Florjańczyk, Z.; Stevens, J. R. *Electrochim. Acta* **1995**, *40*, 2251.
(7) Cheradame, H.; Le Nest, J. F. In *Polymer Electrolyte Reviews*; MacCallum, J., R., Vincent, C. A., Eds.; Elsevier: London, 1987; Vol. 1, Chapter 5.
(8) Abraham, K. M. In *Applications of Electroactive Polymers*; Scrosati, B., Ed.; Chapman and Hall: London; 1993; Chapter 3.
(9) Kelly, I. E.; Owen, J. R.; Steele, B. C. H. *J. Electroanal. Chem.* **1984**, *168*, 467.
(10) Fateaux, D. *J. Electrochem. Soc.* **1988**, *135*, 2231.
(11) Scrosati, B. In *Polymer Electrolyte Reviews*; MacCallum, J., R., Vincent, C. A., Eds.; Elsevier: London, 1987; Vol. 1, Chapter 4.
(12) Borkowska, R.; P?ocharski, J.; Laskowski, J.; Wieczorek, W.; Przy?uski J. *J. Appl. Electrochem.* **1993**, *23*, 991.
(13) Appetecchi, G. B.; Croce, F.; Scrosati, B. *Electrochim. Acta* **1995**, *40*, 991.
(14) Croce, F.; Capuano, F.; Selvaggi, A.; Scrosati, B. *J. Power Sources* **1990**, *32*, 389.
(15) Capuano, F.; Croce, F.; Scrosati, B. *J. Electrochem. Soc.* **1991**, *138*, 1918.
(16) Scrosati, B.; Neat, R. J. In *Applications of Electroactive Polymers*; Scrosati, B., Ed.; Chapman and Hall: London, 1993, Chapter 6.
(17) Sorensen, P. R.; Jacobsen, T. *Electrochim. Acta* **1982**, *27*, 1671.
(18) Such, K.; Stevens, J. R.; Wieczorek, W.; Siekierski, M.; Florjanczyk, Z. *J. Polym. Sci., Polym. Phys. Ed.* **1994**, *32*, 2221.
(19) Boukamp, B. A. *Solid State Ionics* **1986**, *18/19*, 136.
(20) Bruce, P. G. In *Polymer Electrolyte Reviews*; MacCullum, J. R., Vincent, C. A., Eds.; Elsevier: London, 1987; Vol. 1, Chapter 8.
(21) Bailey, F. E., Jr.; Koleske, J. V. *Poly(ethylene oxide)*; Academic Press: New York, 1976; p 115.
(22) Bernson, A.; Lindgren, J. *Solid State Ionics*, **1993**, *60*, 37.
(23) Petersen, G.; Torell, L. M.; Panero, S.; Scrosati, B.; da Silva C. J.; Smith, M. *Solid State Ionics* **1993**, *60*, 55.
(24) Ferry, A.; Jacobsson, P.; Stevens, J. R. *J. Phys. Chem.* **1996**, *100*, 12574.
(25) Grams 386 is a commercially available product from Galactic Industries Corp. Marquardt's nonlinear least-squares-fitting algorithm is used. Marquardt, D. W. *J. Soc. Ind. Appl. Math.* **1963**, *11*, 431.
(26) Mani, R.; Mani, T.; Stevens, J. R. *J. Polym. Sci., Part A: Polym.. Chem.* **1992**, *30*, 2025.
(27) Mani, T.; Mani, R.; Stevens, J. R. *Solid State Ionics* **1993**, *60*, 113.
(28) Peled, E. *J. Electrochem. Soc.* **1979**, *126*, 2047.
(29) Calhoun, A.; Voth, G. A. *J. Phys. Chem.* **1996**, *100*, 10746.
(30) Wieczorek, W.; Zalewska, A.; Raducha, D.; Florjanczyk, Z.; Ferry, A.; Jacobsson, P.; Stevens, J. R. *Macromolecules* **1996**, *29*, 143.
(31) Herr, R. *Electrochim. Acta* **1990**, *35*, 1257.
(32) Mani, T.; Stevens, J. R. *Polymer* **1992**, *33*, 834.